

BEAM DIAGNOSTIC DEVICES FOR A WIDE RANGE OF CURRENTS

P. Strehl

GSI, Gesellschaft für Schwerionenforschung mbH, D-6100 Darmstadt, Fed. Rep. of Germany

**Abstract.**- Efficient operation of flexible heavy ion accelerators depends on the measurement of various beam parameters within a wide intensity range. For the successful implementation and application of computer aided beam optimization procedures a rather elaborate beam diagnostic system becomes essential. Some general considerations for the design of a beam diagnostic system concerning standardization of chambers and elements, as well as discussion of tolerances and alignment procedures will be outlined briefly. The characteristics of some special elements for more universal use like stepping motor driven linear and rotating feedthroughs, compressed air actuators, harps etc. will be presented. Various methods and devices for the measurement and display of beam profiles, emittances in the transverse phase space and beam parameters in the longitudinal phase space will be discussed more in detail. Special reference will be given to signal processing and computer aided beam optimization procedures based on on-line measured beam parameters. On the basis of some typical examples from the Unilac routine operation the capability of a diagnostic system connected directly to processing computers and optimization programs will be demonstrated. Some aspects concerning improvements of beam diagnosis and optimization procedures included in the Unilac upgrading program will be considered.

**1. Introduction.**- Modern accelerators require the availability of relevant beam parameters for computer aided operation. Furthermore, the development of on-line controls and on-line optimization procedures leads to some additional demands, which have to be met by a suitable beam diagnostic system. Therefore the development of versatile measurement techniques became essential in the last years. In comparison to conventional diagnostic systems of older accelerators modern systems may be characterized by the following main demands:

- Movable elements must be remotely controllable and position has to be measurable with appropriate precision by computers.
- Relevant beam parameters must be derived as electrical signals for computer processing and have to cover a broad range of intensities, energies and kind of particles.
- During measurements the destruction of beam has to be minimized.
- Failures of mechanics and accompanying electronics should be detectable by computer.
- Last not least: elements of a diagnostic system should be standardized as much as possible and the main components should be used at the whole facility, including experimental beam lines and diagnostics at the targets. As a consequence elements of the same kind and even different diagnostic elements should be exchangeable along the accelerator.

In the following a short survey on beam diagnostics will be presented, including the description of some signal processing procedures and the on-line signal evaluation by computers. Although contributions are derived mainly from the Unilac the characteristics of the selected elements and applied procedures fit to cyclotrons and other rf-accelerators, too.

**2. Standardization.**- Standardization starts with the simple design of chambers. Fig. 1 shows a fully equipped chamber as typical at the Unilac

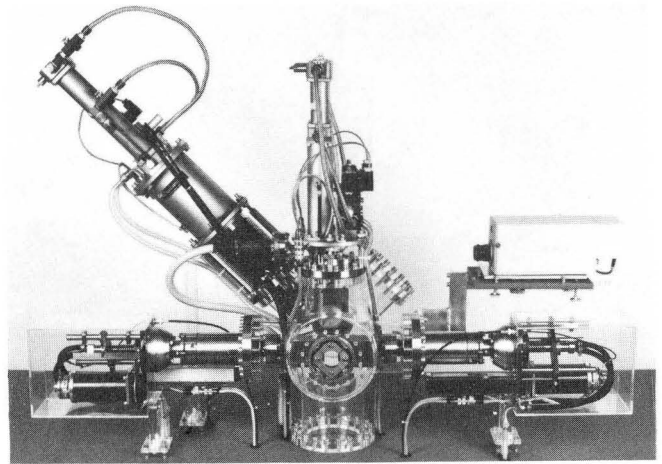


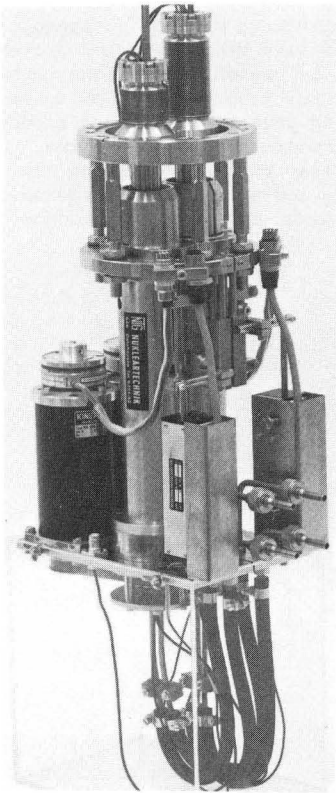
**Fig. 1:** Typical diagnostic chamber equipped with: slits, Faraday-cup, harp, viewing screen, segmented aperture.

The distance between supporting flanges and beam axis should be unified after an optimization with respect to the various elements which have to be fitted. As a consequence universal elements as for example compressed air actuated feedthroughs may be designed with the same stroke and will be exchangeable along the accelerator. For the same reasons supporting flange dimensions should be unified and fit to a commercially available product. Tolerances of manufacturing with respect to parallelism of flanges, angular deviations and accuracy of relevant dimensions should be fixed as small as possible taking manufacturing prices into account.

The advantage becomes evident in cases of maintenance or exchange of elements if once all chambers are aligned correctly to beam axis.

For the same reasons diagnostic elements which have to be assembled to the chambers should be manufactured with small tolerances, too. In addition, all available devices have to be adjustable within reasonable limits. Therefore diagnostic elements which have to be installed later on into the beam lines can be aligned using a standard stand-by chamber without time consuming alignment procedures at the accelerator itself.

Besides standardized vacuum chambers some elements of universal use should be available for the assembling of various beam diagnostic devices. Fig. 2 shows a stepping motor driven feedthrough and gives the main specifications. The device exists also as a single version as used for emittance measurements (see fig.14).



Sealing:  
CF 100,  
membran bellows

Drive:  
2 x 1.8° stepping  
motors

Displacement:  
0.03 mm/step

stroke:  
40 or 80 mm

Fig. 2: Stepping motor driven feedthrough (double version).

The double version of compressed air actuator as shown in fig. 3 can be also modified very easily to a single version. In addition, a similar unit exists, which can supply cooling to the attached elements.

Another element of universal use is the rotatable compressed air actuator as shown in fig. 4.

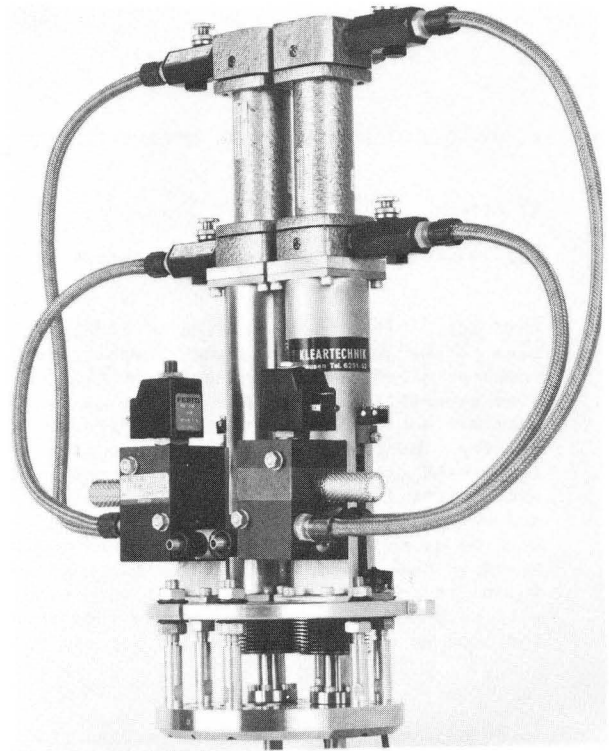


Fig. 3: Compressed air actuator (double version).

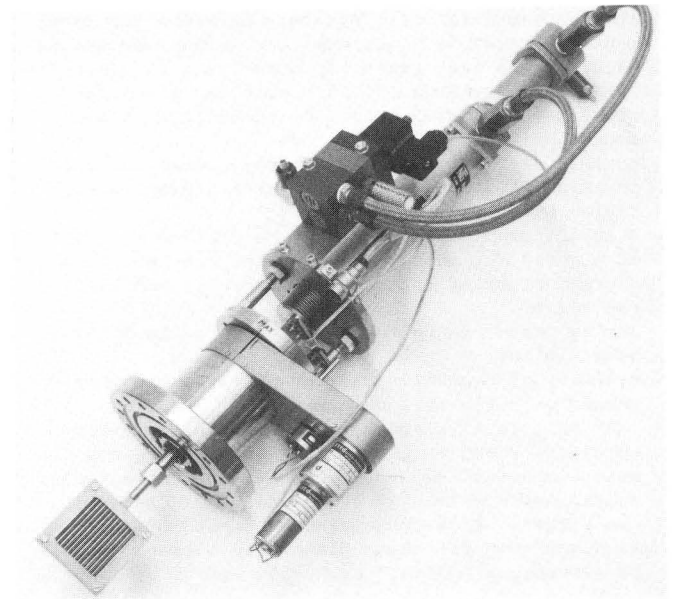


Fig. 4: Rotatable compressed air actuator equipped with beam attenuating rods.

### 3. Diagnostics elements and measurement techniques.-

Harps: A collection of various harps, which can be mounted on a single compressed air actuator is shown in fig. 5. Besides the simple use of harps for visual observation of beam profiles some measurement algorithms using the computing capability of an on-line process control system will be useful for tuning up an accelerator. The use of harps for on-line beam alignment is described in ref. 1,2. Important conditions for full application of profile harps are suitable electronics

and computer procedures for the application of mathematical descriptions. Fig. 6 shows a simplified block diagram of harp electronics.

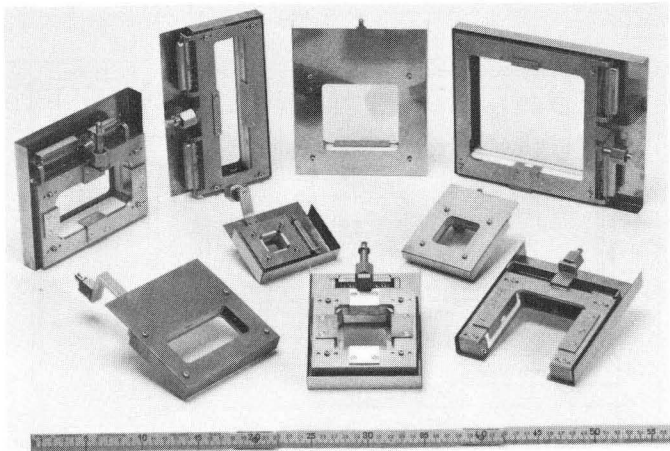


Fig. 5: Harp collection.

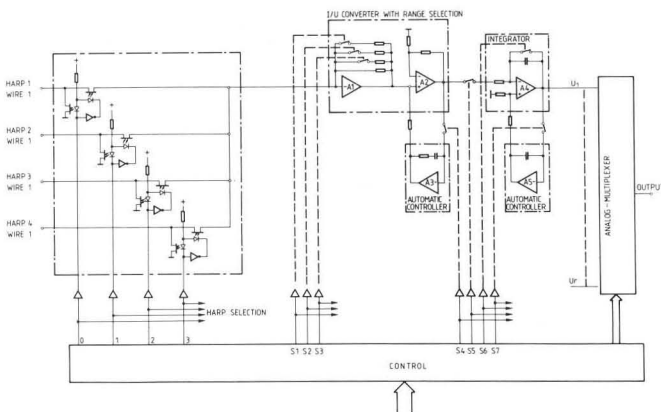


Fig. 6: Simplified block diagram of harp electronics. Sensitivity: 500 mV/nA, dynamic range: 1 : 10<sup>4</sup>, CMR: ≥ 50 dB, OPTO-FET: 300 MΩ/300 Ω.

Besides an improvement concerning sensitivity (see ref. 3) a FET-multiplexer system has been added in front of the I/U-converters for computerized fast switching. The advantage for visual beam alignment is evident.

The addition of an automatic off-set compensation circuit improves the electronics considerably. Applying fit procedures<sup>4</sup> to the measured points a mathematical description of profiles can be obtained.

An emittance measurement can be performed by measuring the profile variation on one grid in dependence of the transfer matrix in front of the grid. The procedure is explained schematically in fig. 7. Referring to the notation as given in ref. 5 the following relations for the transformation of the ellipse parameters  $\alpha, \beta, \gamma$  hold:

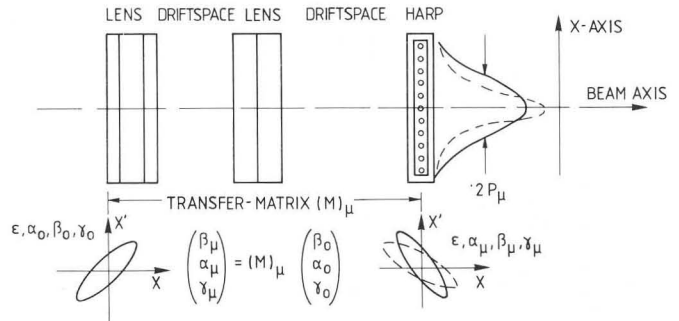


Fig. 7: Determination of emittance parameters by profile measurement and quadrupole variation.

$$\begin{bmatrix} \beta \\ \alpha \\ \mu \end{bmatrix} = \begin{bmatrix} C^2 & -2CS & S^2 \\ -CC' & CS' + SC' & -SS' \\ C'^2 & -2C'S' & S'^2 \end{bmatrix} \begin{bmatrix} \beta_0 \\ \alpha_0 \\ \mu_0 \end{bmatrix}$$

With C, S, C', S' defined by

$$\begin{bmatrix} X \\ X' \end{bmatrix} = \begin{bmatrix} C & S \\ C' & S' \end{bmatrix} \begin{bmatrix} X_0 \\ X'_0 \end{bmatrix}$$

The measured profile width (2P) is related to  $\beta$  by  $\sqrt{\epsilon\beta} = P$ . The unknown values  $\alpha_0, \beta_0$  and  $\epsilon$  can be determined by measuring the profiles in dependence of 3 different quadrupole settings, taking into account  $\beta\gamma - \alpha^2 = 1$ . Obviously more than one quadrupole may be involved in the variation procedure since the whole transfer matrix can be determined.

The procedure is very sensitive to the accuracy in determining P so the algorithm may be improved by measuring the dependence  $P_\mu = f(M_\mu)$  for a set larger than 3 and taking the whole set of measured points into account. Applying a least squares fit to the relation

$$S = \sum_{\mu} [P_\mu^2 - [C_\mu^2 \beta_0 \epsilon - 2C_\mu S_\mu \alpha_0 \epsilon + S_\mu^2 \mu_0 \epsilon]]^2$$

determination of  $\alpha_0, \beta_0, \gamma_0, \epsilon$  is straightforward and results from

$$\frac{\partial S}{\partial(\beta_0 \epsilon)} = 0, \quad \frac{\partial S}{\partial(\alpha_0 \epsilon)} = 0, \quad \frac{\partial S}{\partial(\mu_0 \epsilon)} = 0$$

and  $\beta_0 \gamma_0 - \alpha_0^2 = 1$ .

Fig. 8 shows an example of emittance displays using this procedure including a transformation of ellipses, to a selected position along the beam line. Really the described procedures have to be tested more in detail by experiments, since as practice has shown sometimes the obtained solutions of the equations are imaginary. Inaccuracies of profile measurement and inconsistencies in the on-line determination of the transfer matrix must account for the discrepancy.

Harps may be used effectively for the fast measurement of charge state distributions behind strippers. Since most of accelerator facilities combine a stripper with a charge state separation system a simple profile measurement in the dispersion plane of the charge state separation system may substitute time consuming scanning procedures.

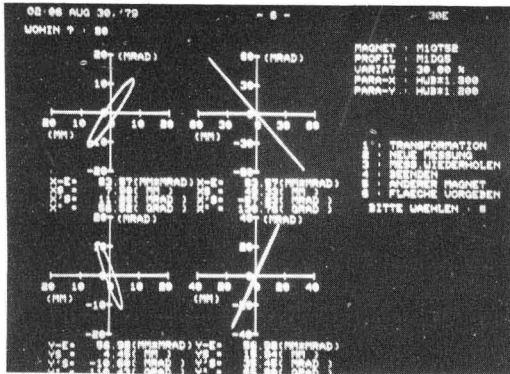


Fig. 8: Emittance ellipses determined from profile measurements (see text).  
Left: measured emittances, right: transformation along the beam line based on on-line read out of quadrupole settings.

Fig. 9 shows the arrangement at the Unilac. A large profile grid was installed on the left hand side of the charge state separation chamber. The grid consists of 62 vertically aligned tungsten-rhenium wires with a thickness of 0.1 mm.

15:36 FEB 02, '81 - 5 - 30ABC ,CPR  
A B C - U N I L A C - E I N S T E L L H I L F E N  
ORTSDISPERSION : 5.43 MM/PROZENT IMPULSABWEICHUNG  
IMPULSABWEICHUNG = (E-DEH)/SEH  
WELCHE LADUNG SOLL IN DIE EH ? : 40  
ABSTAND ZWISCHEN LADUNGEN 40 - 41 BZW 39 - 40 = 13.57 MM  
PRUEFE SCHLITZBREITE 7L - 7R (S4DS8) !

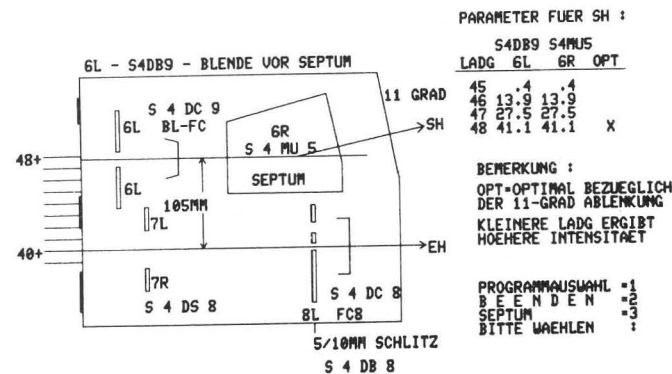


Fig. 9: Schematic computer plot of the charge separation chamber of the Unilac.

The distance between the wires was optimized taking into account:

- the characteristics of the Unilac charge state separation system,
- the required resolution,
- the necessary range of profile measurement.

A spacing of 2 mm was selected, giving about 6 - 7 measurement points even in the worst case of uranium 40+ at 1.4 MeV/u. The range is about 120 mm, which is

sufficient to display the relevant part of the charge state distribution at once for all kind of ions. The block diagram of the signal processing electronics is shown in fig. 10.

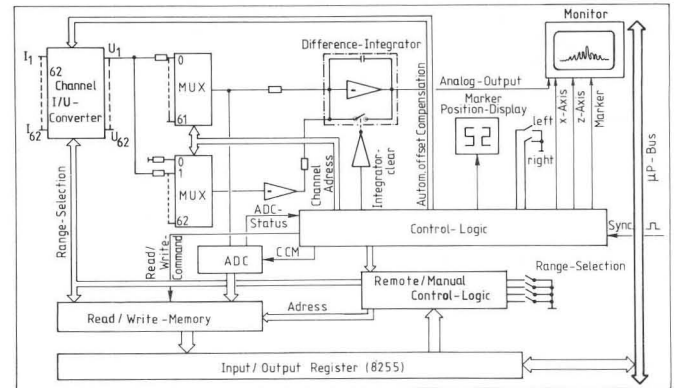


Fig. 10: Control electronics for the measurement of charge state distributions by a profile grid.

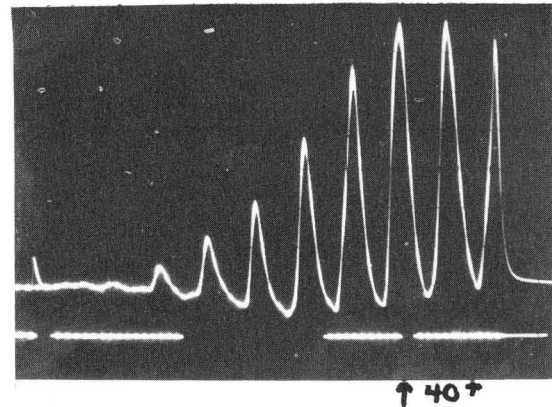


Fig. 11: Charge state distribution behind the stripper measured with the profile grid at fixed magnetic field of the analyzing system.

Smooth lines in the oscillogram of fig. 11 are provided by the difference integrator (see fig. 10) which interpolates between channels. For comparison a spectrum taken by computer using a scanning procedure is shown in fig. 12. Interfacing the electronics to the computer in near future will combine the very fast profile measurement with the comfort of an automatic evaluation of measured profiles, including fits for the exact determination of charge numbers even for unknown elements.

In some cases rotating wire scanners may be preferred for profile measurements. The main advantages of scanners are:

- In general a higher loss of beam power can be tolerated on account of the duty factor generated by the rotating motion of the scanning wire.
- Falsifications of profiles due to changes in secondary emission coefficient during the lifetime of the wire are minimized.
- Electronics for profile signal processing can be cheaper since there is only one channel.

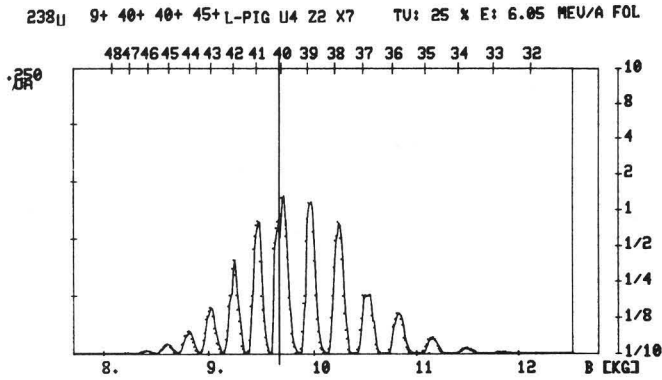


Fig. 12: Computer display of charge state distribution behind the stripper including a spline fit to the measured points obtained by scanning the magnetic field.

On the other hand electronics for the correct determination of wire position may be more complicated. In case of pulsed beams further complications may arise from the demand of exact synchronization. Harps should be preferred for profile measurements, if the advantages of a wire scanner mentioned above are of no significant importance. Fig. 13 shows the main parts of a scanner used at GSI.

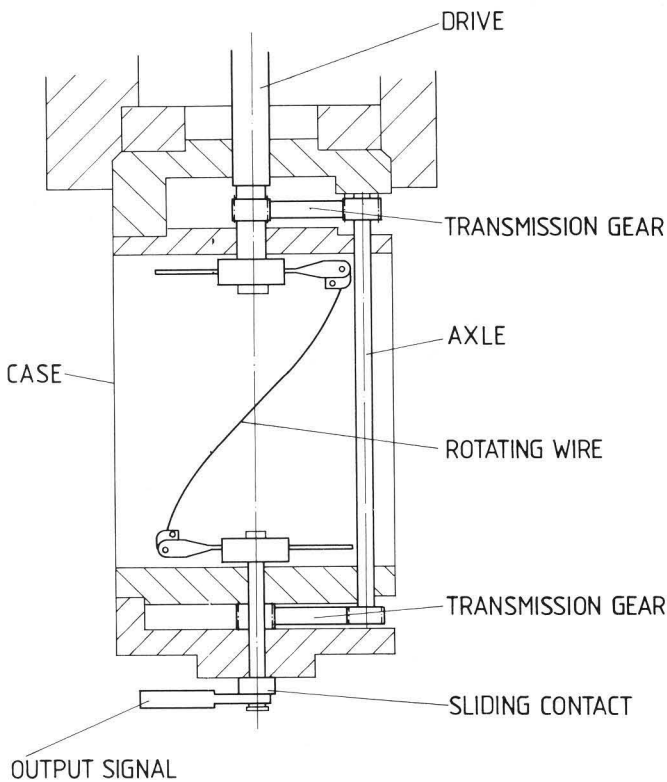


Fig. 13: Rotating wire scanner.

4. Emittance measurements.- Devices used at various accelerators and described in literature are of great diversity. Three different schemes based on the same principle using linear feedthroughs for the stepwise motion of slits and detectors are shown in fig. 14.

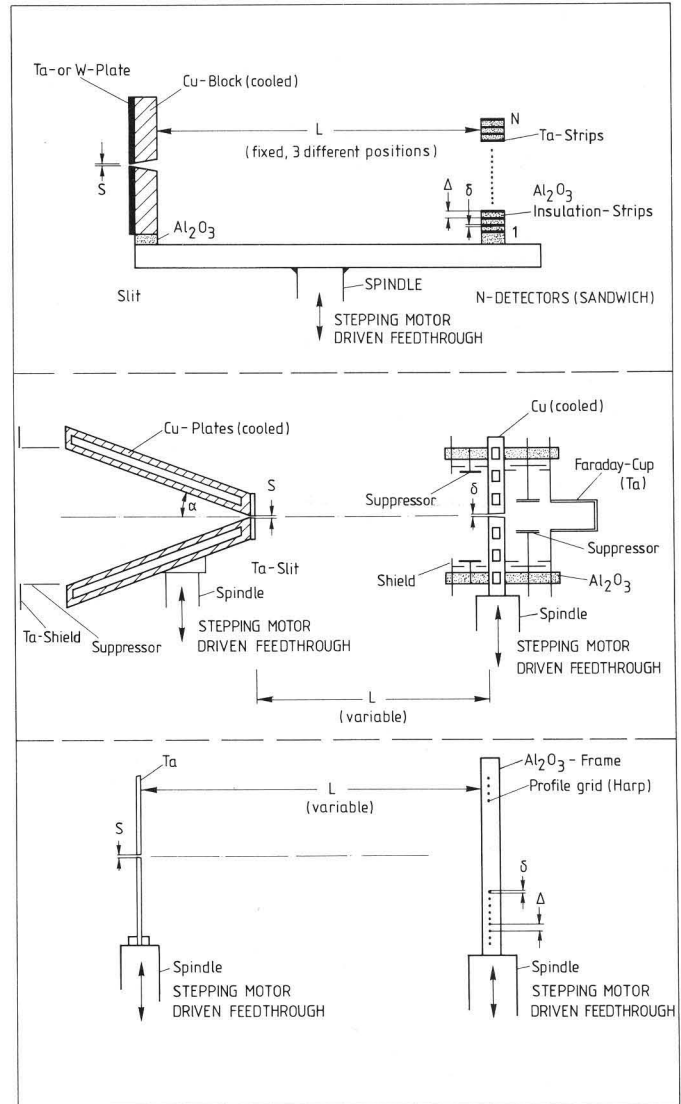


Fig. 14: Principles of emittance measurements using linear feedthroughs.

The devices can cover a broad range of parameters with respect to beam power, resolutions and ranges in position and angular, respectively. The upper device in fig. 14 can be very compact using only one stepping motor driven feedthrough. Although resolution and range are limited by mechanical dimensions they may be changed within given limits by mounting the detector head at different distances with respect to the slit. But it is evident, that any change of detector position will change range and resolution in determined ratios.

The scheme in the middle of fig. 14 can be used especially for high beam powers (up to 25 kW, 10 kW/cm<sup>2</sup>). Even the second slit in front of the scanning Faraday cup is provided with cooling. Resolutions and ranges in transversal phase space depend mainly on the minimum step sizes and the stroke of the feedthrough and may be optimized by software using a  $\mu$ P-controlled electronics. The great flexibility on account of the second independent feedthrough offers the possibility of emittance measurements even for considerably misaligned beams. The distance between the first slit and the detector may be changed without mechanical restrictions. Since there is only one detector for the profile determination

measurement time will increase considerably in comparison to multidetector devices.

Finally the scheme shown on bottom of fig. 14 combines some advantages of both devices discussed above if intermediate steps for the position of the grid as well as "off-set" positions with respect to the slit are considered. Fig. 15, 16 give examples of displays performed by computer evaluation of measured data.

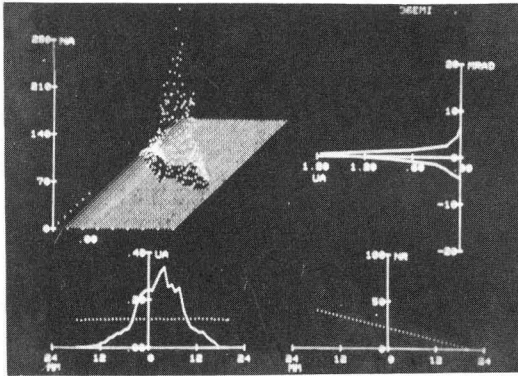


Fig. 15: Display of emittance measurement data. Top left: original measured points, bottom left: beam profile, top right: angular profile, bottom right: stepping motor positions.

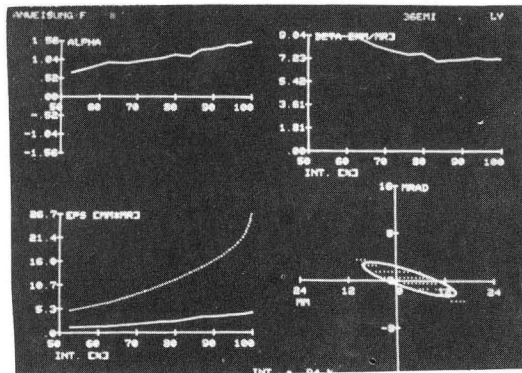


Fig. 16: Display of calculated emittance ellipse parameters in dependence of percentage.

The applied algorithm for the determination of emittance parameters in dependence of percentage of beam may be of interest. The volume of small rectangular cylinders may be defined by

$$V_{xx'}(I) = \Delta x \cdot \Delta x' \cdot I_{xx'}$$

where

- $\Delta x$  = stepwidth in slit position
- $\Delta x'$  = angular resolution
- $I_{xx'}$  = measured intensity for the corresponding positions of slit and detector.

Summing up the  $V_{xx'}(I)$  by neglecting contributions with  $I_{xx'}$  below a fixed threshold (mainly determined by the quality of the signal processing electronics) leads to a good approximation for the volume integral

$$V_{\max} = \int dx dx' dI_{xx'}$$

representing 100 % of beam. On the other hand cross sections through the display in fig. 18 (top, left) parallel to the  $x, x'$ -plane will result in ensembles

of points located within the boundaries defined by the shape of the figure. Applying a suitable ellipse fit leads to the emittance areas for each cross section. Percentage of beam results from a summation over all  $V_{xx'}$  within the boundary divided by  $V_{\max}$ .

Emittance measurements of high precision combined with on-line control of quadrupole settings and powerful software may result in very efficient optimization procedures as described for example in ref. 1,2. Based on the usefulness of emittance measurements one of the conventional systems was modified to allow very fast displays of envelopes.

Normally emittances are measured by moving a slit-detector system as shown in fig. 14 (top) step by step through the beam. Conserving this possibility for high precision measurements the additional option for a fast beam deflection is explained schematically in fig. 17.

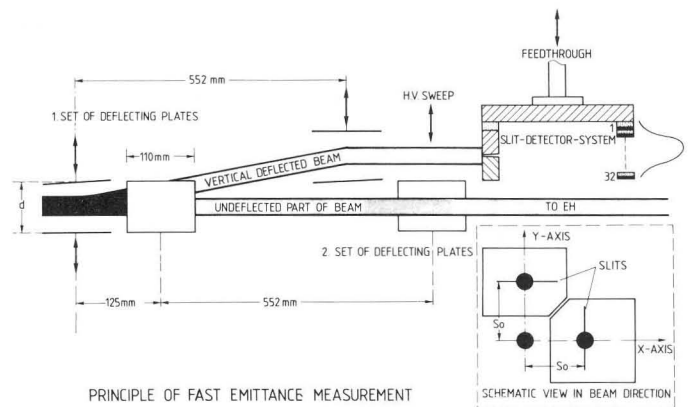


Fig. 17

In a new designed large vacuum chamber two sets of deflecting plates mounted on 4 double high vacuum feedthroughs (see fig. 2) were installed. For fast measurements two orthogonal standard slit-collector systems are positioned parallel to the beam line as shown in fig. 17. A microprocessor controlled electric deflecting voltage sweeps the beam by a staircase function. The relevant system parameters are summarized in the table.

DEFLECTING VOLTAGE	
MINIMUM	: 9 200V
MAXIMUM	: 18 500V
INCREMENTS	: 300V
MINIMUM TIME/INCREMENT	: 1ms
RANGES	
POSITION ( $X_{\max}, Y_{\max}$ )	: $\pm(75-25)$ mm
ANGLE ( $X'_{\max}, Y'_{\max}$ )	: $\pm 16$ mrad
CURRENT/DETECTOR STRIP	: 10nA-100µA
RESOLUTION	
POSITION ( $\Delta x, \Delta y$ )	: 0.1mm
ANGLE ( $\Delta x', \Delta y'$ )	: 1mrad
STEP WIDTH IN POSITION	: (0.5-1.6) mm

Fig. 18 shows a block diagram of the  $\mu P$ -control electronics. The minimum refresh time for a complete emittance display as shown in fig. 19 is 0.25 s for one plane. The ratio between deflected and undeflected part of the beam can be varied within broad ranges. A more detailed description is given in ref. 6.

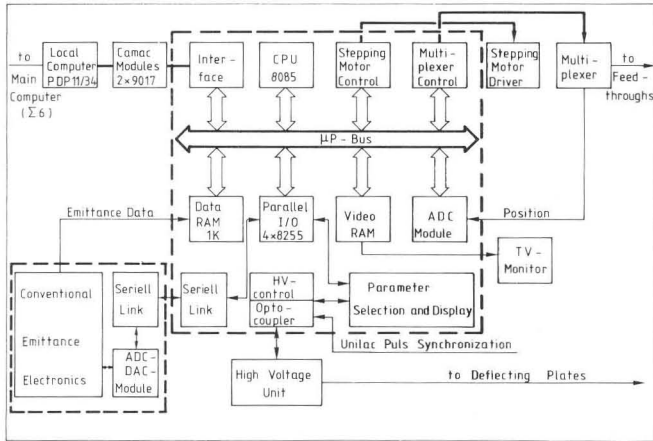


Fig. 18: Microprocessor control electronics for fast emittance measurements.

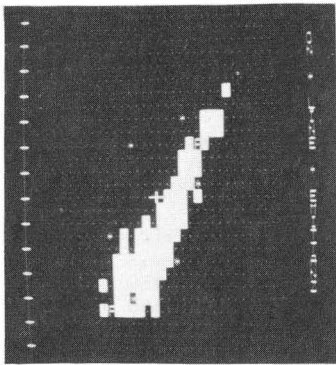


Fig. 19: Fast emittance display on a TV-screen provided by the Video-RAM.

5. Capacitive pick up's.- Applications of capacitive pick up's for measurements in the longitudinal phase space have been reported in ref. 3,7,8. Most of the described procedures will be practicable at rf-accelerators. The probe geometrie has to be optimized with respect to the rf-parameters and expected bunch structure.

One first step in the design of a diagnostic system based on capacitive pick up's has to be an estimation of the expected signal strengths. Therefore the required minimum numbers of particles (charge state = 1) within one accelerated bunch has been computed for typical conditions and plotted against energy in fig. 20. The given limits for  $(N_e)_{min}$  are based on a computer calculation according to ref. 8. An influenced electrical signal of  $15 \mu V$  at 50 Ohms was assumed, giving a signal to noise ratio of 1:1 for a typical 1.5 GHz broadband amplifier as developed at GSI<sup>8</sup>. The figures for  $(N_e)_{min}$  may be decreased by considering also resonant systems. But, keeping in mind the loss of information, broad band systems are more versatile and should be preferred.

Remembering<sup>8</sup> that for cylindrical probes

$$i = \frac{d}{dt} \epsilon_0 \int E_{\perp} 2\pi R dz, \quad (1)$$

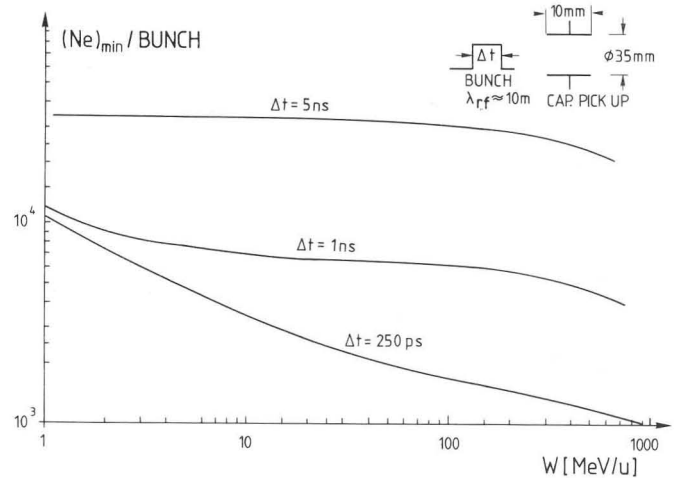


Fig. 20: Minimum numbers of particles for capacitive pick up measurements (see text).

where

$i$  = influenced current;

$E$  = transversal component of the electrical field generated by the bunch;

$R$  = probe radius;

$z$  = longitudinal coordinate;

a rough approximation of signal strength may be obtained by Gaussian theorem:

$$q = \epsilon_0 \int \vec{E} dF \quad (2)$$

Replacing  $\frac{d}{dt}$  in the relation  $i = \frac{d}{dt} q$  by  $1/\Delta t$  leads to an useful estimation for  $i$  as given in equ. (1):

$$i \approx \frac{160 pA}{\Delta t [ns]} \cdot K \frac{L}{\beta c \Delta t} \cdot \frac{2\pi R L}{2\pi R L + 2\pi R^2}, \quad (3)$$

where  $L$  = probe length.

The meaning of the separated terms is evident. In equ. (3) a factor  $k$  was introduced to consider the influence of particles yet outside of the probe volume as defined by equ. (2). Experience leads to  $k \sim 2$  for bunch lengths  $\beta c \Delta t \gg L$ . On the other hand for very short bunches defined by  $\beta c \Delta t \ll L$  the product  $k \cdot \frac{c}{\beta c \Delta t}$  should be replaced by 1. From the deduced relation also the dependences of  $i$  from the parameters, are described in an approximate way.

Experimental programs at modern accelerator facilities mostly demand variable energy, therefore a good energy measurement system becomes essential. The optimization of a time of flight (TOF) measurement as discussed in ref. 8 and explained schematically in fig. 21 may be facilitated by means of fig. 22. In fig. 22 the obtainable accuracy  $\Delta W/W$  has been plotted for somehow typical conditions of an 30 MHz rf-accelerator.

An application of TOF-techniques is the very precise calibration of injection energy if there two bunchers in front of a capacitive pick up are available. If only one buncher is available, a precise time reference signal must be supplemented.

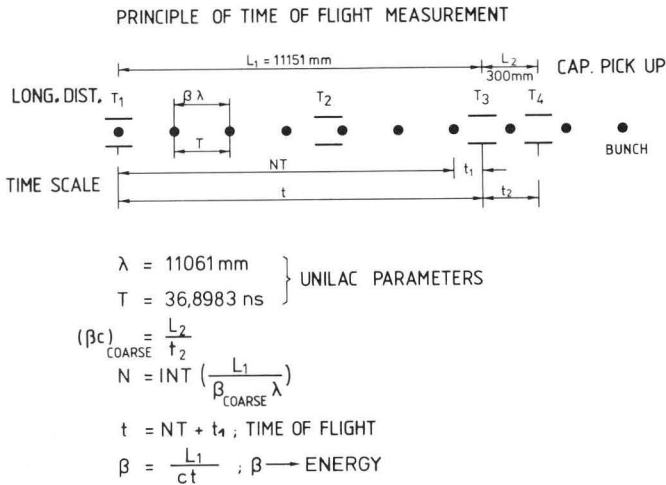


Fig. 21

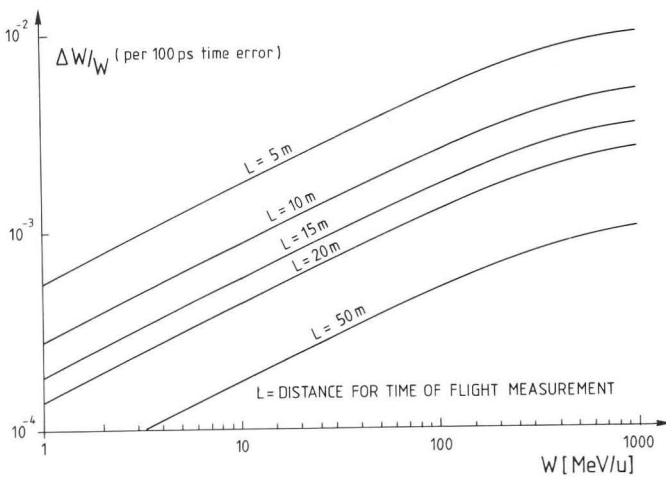


Fig. 22: Accuracy of TOF-measurements.

The principle is explained in fig. 23 on the base of Unilac parameters. Since  $\beta\lambda$ -values are very small at the Unilac injection energy of 11.6 keV/u the precision which can be achieved becomes very high. It is evident that also the accuracy of the coarse measurement must be relatively high. Taking into account the supplied calibration of modern dc high voltage power supplies will be better than 1 % a coarse measurement may be omitted. Once the calibration has been performed the exact phase difference of the double buncher system can be calculated.

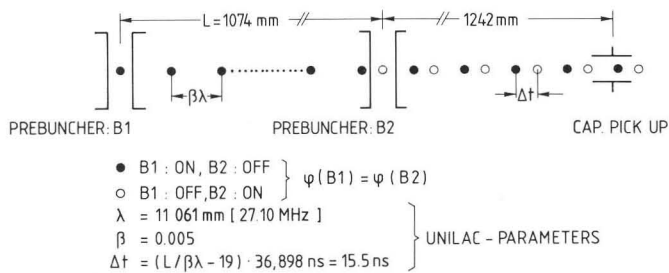


Fig. 23: Calibration of injection energy by TOF-techniques.

As discussed briefly in ref. 7,8 capacitive pick up's can be used for the detection of ion source plasma oscillations or similar effects. A simple signal processing electronics as shown in fig. 24 has been developed for the purpose of ion source parameter optimization (see fig. 25).

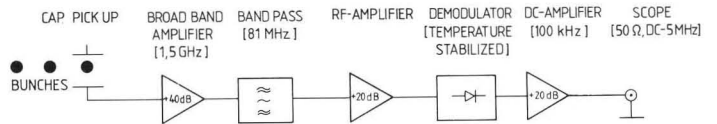


Fig. 24: Simple electronics for the observation of ion source oscillations (see text).

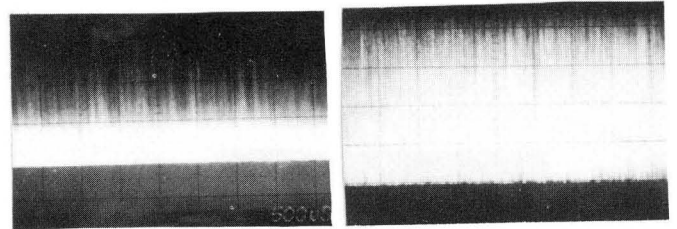


Fig. 25: Detection of ion source plasma oscillations. Left: poor settings of ion source parameters, right: optimized. Scale: 500  $\mu\text{s}/\text{Div}$ .

Another simple electronics shown in fig. 26 can be helpful for the evaluation of beam quality in longitudinal phase space. It offers the possibility to display single bunch signals or small groups of them on a fast oscilloscope. Taking advantage of the variable delay against a time reference signal TOF-measurements may be performed in dependence of the delay looking for transient effects or instabilities of rf-power amplifiers (see fig. 27).

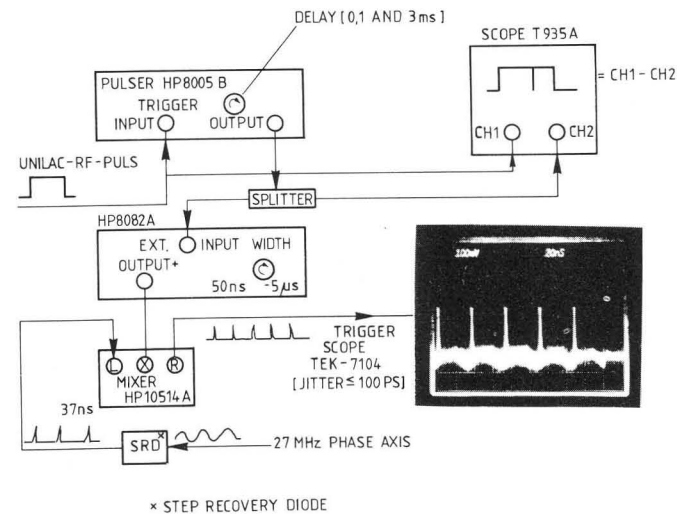


Fig. 26: Special trigger circuit for the observation of single bunches (see text).



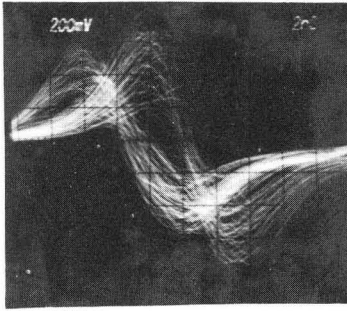


Fig. 27: Diagnosis of transient effects and rf-instabilities by TOF-techniques. Left signal group corresponds to the first part of rf-pulses, right group to the middle of rf-pulse.

A further extension of applications for capacitive pick-up's will be the determination of emittance ellipses in the longitudinal phase space. The resulting arrangement can be seen in fig. 28.

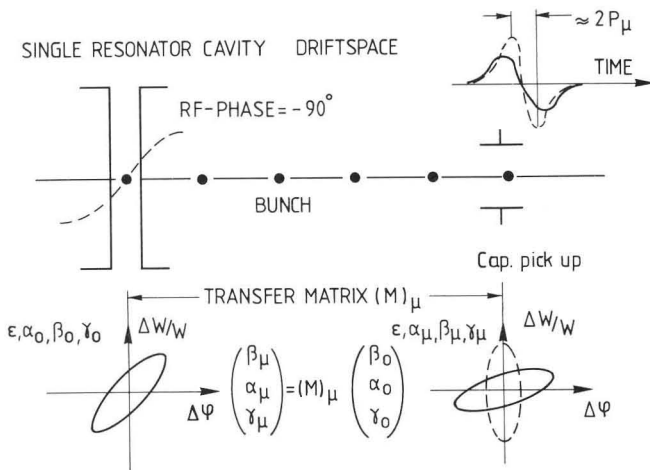


Fig. 28: Scheme of emittance measurements in longitudinal phase space.

Adding a second capacitive pick-up to the scheme in fig. 28 also a TOF-measurement may be accomplished and therefore the calibration of the rf-cavity can be performed simultaneously. Up to now no practical experience has been gained since the corresponding computer program will be implemented just now and may be tested after the Unilac upgrading program will be finished.

6. Faraday-cups.- Faraday cups are very simple in design if there are no problems with respect to beam power, sputtering, space charge, secondary particle suppression and contact potentials. Fig. 29 shows the lay-out of a cup which was designed for beam power densities up to 10 kW/cm<sup>2</sup> - using graphite covers on copper cooled supporting blocks. 40 MeV protons will be stopped completely in the graphite minimizing radio-activation of materials.

The characteristics and usefulness of coaxial Faraday cups have been discussed in ref. 7. A disadvantage of the original GSI-design may be the small diameter of the stopping plate. The new design is shown in fig. 30. Considering the aperture of 50 mm the device can be used for broadband measurements as well as for dc beam current measurement.

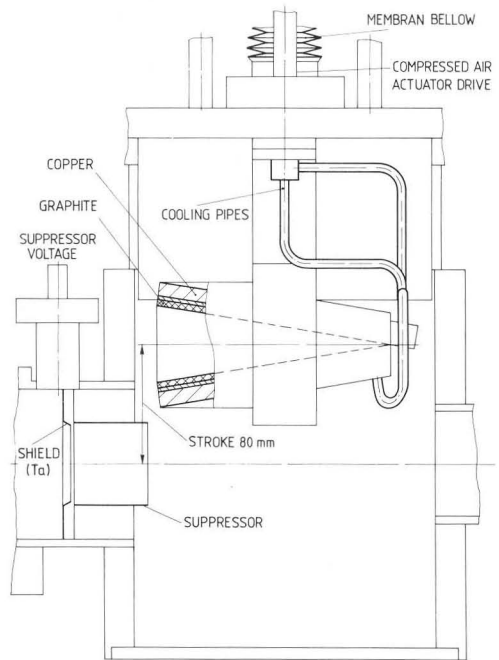


Fig. 29: High power Faraday cup.

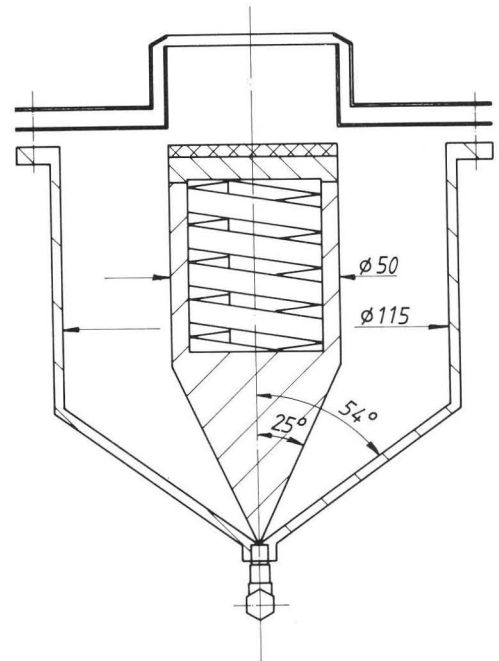


Fig. 30: New designed head of a Faraday cup provided for measurement of mean current and broad band signal observation.

The cup will stop particles with a range of up to 5 cm in copper and is designed for beam powers up to 20 kW.

7. Conclusion.- In the last years the development of modern beam diagnostics has gone in parallel with computerization of accelerator control. As a consequence pure visuall observation has been replaced or supplemented by more sophisticated methods. Certainly the

next decade of beam diagnostics and accelerator control will be characterized by developments of more on-line optimization procedures.

8. Acknowledgement.- The author wishes to acknowledge the work of H. Kraus, J. Störmer and C. Hoffmann in the mechanical design of diagnostic elements. Development of electronics and experiments for testing would not have been possible without the assistance of the Unilac operations group. On-line optimization procedures were worked out in collaboration with J. Klabunde. Most of complex computer programs are written by V. Schaa.

9. References.-

<sup>1</sup>L. Dahl et al., "Longitudinal and Transverse Beam Optimization at the Unilac", 1979 Linear Accelerator Conference, Montauk, N.Y., BNL 51134, p. 291.

<sup>2</sup>L. Dahl, "Computer-Aided Tuning Procedures at the Unilac", these proceedings.

<sup>3</sup>J. Glatz et al., "Some Aspects of the Unilac Beam Diagnostic System", 1976 Proton Linear Accelerator Conference, Chalk River, AECL-5677, p. 306.

<sup>4</sup>V. Schaa, "Emittance Measurements with Profile Grids", Thesis, TH-Darmstadt, 1978.

<sup>5</sup>K.G. Steffen, "High Energy Beam Optics", Wiley, N.Y. 1965.

<sup>6</sup>P. Strehl et al., "A New Emittance Measuring Device at the Unilac", 1981 Particle Accelerator Conference, Washington, D.C., ISSN 0018-9499, p. 2216.

<sup>7</sup>J. Klabunde et al., "Measurements of Energy, Energy Spread and Bunch Width at the Unilac", 1979 Linear Accelerator Conference, Montauk, N.Y., BNL 51134, p. 297.

<sup>8</sup>P. Strehl et al., "The Phase Probe Measuring System at the Unilac. Probe Dimensioning and Signal Evaluation", GSI 79-13, Dec. 1979, Internal Report, translated by: Leo Kanner Associates, Redwood City, CA 94063, Dec. 1980.

" DISCUSSION "

D. LIND : Have you tried inductive time pickoffs ?  $\beta$  for heavy ions generally is low  $< 0.2$  so capacitive pickoff is preferred.

P. STREHL : No, for our needs, capacitive is preferred.

H.W. SCHREUDER : What is the overall risetime of your capacitive pick-up system, including amplifier and cabling ?

P. STREHL : About 300 ps, it is influenced by the probe length (should be  $\beta c \Delta t$ ), by the quality of cables (should be Spiroline or Flexwell) and the amplifier (should have 1.5 GHz or more).